Analytical and Bioanalytical Chemistry
https://doi.org/10.1007/s00216-020-02850-y

RESEARCH PAPER

Sensitive detection of microRNA using a label-free copper nanoparticle system with polymerase-based signal amplification

Jiangnan Lu[1] · Shuping Liang[1] · Li Tan[1] · Kun Hu[1] · Shulin Zhao[1] · Jianniao Tian[1]

Received: 19 October 2019 / Revised: 21 July 2020 / Accepted: 27 July 2020

Abstract

The abnormal expression of microRNAs (miRNAs) has been reported in many diseases, so it is of great interest to develop simple and accurate methods for the detection and analysis of miRNA expression. We have developed a novel biosensor to detect miRNAs. This method is based on a polymeric double-stranded DNA (dsDNA) copper nanoparticle (CuNP) template that is synthesised by a polymerase. When Cu^{2+} and ascorbic acid are added to the system, the dsDNA template (which is rich in A-T bases) promotes the formation of CuNPs, resulting in high fluorescence intensity. This system provides sensitive analysis of miRNA expression with a limit of detection down to 17.8 pmol/L, due to significant changes in the fluorescence signal of the system before and after the addition of the target. The linear range between F_0-F and concentration of miR-122 is 80.0 pmol/L to 4.50 nmol/L, and the recovery rate in spiked HepG2 cell lysates is 93.33–102.53%. This method expands the applications of fluorescent DNA-CuNPs in the field of biosensor analysis, and can be used to detect and analyse any miRNA marker by changing the target recognition sequence.

Keywords MicroRNA · Enzymatic polymerisation · Copper nanoparticles · Ascorbic acid

Introduction

MicroRNAs (miRNAs) are small, endogenous, non-coding, single-stranded deoxyribonucleotide molecules that are ubiquitous in eukaryotes [1, 2]. They possess great potential as a biological marker for the detection of diseases, especially cancer [3–5]. For example, elevated miRNA-122 expression is closely associated with hepatitis, liver cancer, lung cancer, and other common diseases [3, 6–8]. As the incidence of cancer increases, there is an urgent need for advanced detection methods for miRNA biomarkers in vivo. Because of the low abundance and instability of miRNA in biological samples, constructing a sensitive, selective, and quantitative analysis method is challenging.

In order to address this challenge, researchers have developed a number of nucleic acid signal amplification techniques for the sensitive detection of miRNAs [9–12], such as polymerase chain reaction (PCR) [13, 14], rolling circle amplification (RCA) [15–18], hybridisation chain reaction (HCR) [19–22], strand displacement amplification (SDA) [23], and other methods [10, 24–26]. These methods are novel in design, with satisfactory sensitivity and selectivity. For instance, Chu et al. [17] first reported a target-induced RCA (TPRCA) strategy to visualise miRNA levels in single cells with high sensitivity and selectivity. However, the above methods are costly and usually require labelling with fluorophores or intercalating dyes and specialised equipment.

In recent years, metal nanoparticles (MNPs) with strong fluorescence emission have attracted interest as a substitute for common organic dyes [6]. MNPs widely used as biological sensors include gold nanoclusters (AuNCs) [27, 28], quantum dots (QDs) [29–31], carbon quantum dots (CQDs) [32], silver nanoclusters (AgNCs) [33], and copper nanoparticles (CuNPs) [34–37]. Among these nanomaterials, AuNCs, QDs, CQDs, and AgNCs take a long time to prepare, with complicated steps and strict requirements for the reaction environment. By contrast, CuNPs are extremely cost-effective nanoparticles with a large Stokes shift [11], low toxicity, good

Electronic supplementary material The online version of this article (https://doi.org/10.1007/s00216-020-02850-y) contains supplementary material, which is available to authorized users.

✉ Jianniao Tian
birdtjn@sina.com

[1] Key Laboratory for the Chemistry and Molecular Engineering of Medicinal Resources (Ministry of Education of China), School of Chemistry and Pharmaceutical Science of Guangxi Normal University, Guanxi, Guilin 541004, China

Published online: 12 August 2020

biocompatibility, fluorescence emission that is adjustable in the synthesis process, and controllable formation through the length of DNA templates, making CuNPs very suitable for detection of complex biological matrix targets. Moreover, DNA-templated CuNPs have strong fluorescence emission, and have been implemented as a multifunctional DNA detection strategy for biosensing analysis [11, 28, 34–38]. For instance, Tang et al. reported a novel biosensing strategy that achieves ultrasensitive detection of miRNA using T7 exonuclease to regulate CuNP templates [39]. Miao et al. developed a click reaction based on CuNPs to detect alkaline phosphatase [40]. He et al. utilised double-stranded DNA (dsDNA)-CuNPs to construct a novel and intelligent composite reagent that can be exploited for hydrogen peroxide detection [41].

In this study, we developed a simple, fast, label-free biosensor for miRNA, by utilising polymerase to form a long dsDNA-templated copper nanoparticle. When the miRNA target is not present, the SDA reaction is inhibited and the fluorescence intensity is very low. However, when the target is present, the SDA reaction is initiated and the RNA/DNA complex is circulated at the same time to produce a long dsDNA template. Finally, a large number of CuNPs form along the long dsDNA template, and these emit intense fluorescence in the presence of ascorbic acid. This method can achieve rapid and sensitive detection, as demonstrated by significant changes in fluorescence intensity after the addition of a target miRNA. Furthermore, the method can detect any miRNA by incorporating different target recognition sequence DNA [42].

Materials and methods

Materials and reagents

Tris(hydroxymethyl) aminomethane (Tris) and Agarose G-10 was purchased from Sigma (Spain). Sodium chloride (NaCl) and magnesium acetate ($Mg(Ac)_2$) were purchased from Huawei Ruike Chemical Co., Ltd. (Beijing, China). Boric acid (H_3BO_3) and edetate disodium (EDTA) were purchased from Sinopharm Chemical Reagent Co., Ltd. (Shanghai, China). Klenow fragment ($3' \rightarrow 5'$ exo) (KF) was purchased from New England Biolabs (USA). Copper sulfate ($CuSO_4 \cdot 5H_2O$) and 3-(N-morpholino)propanesulfonic acid sodium (MOPS) were purchased from Yinuokai Technology Co., Ltd. (Beijing, China). Fetal bovine serum (FBS) was purchased from Shanghai ExCell Bio (Shanghai, China). All reagents were analytical grade, and the water used was diethyl pyrocarbonate-treated (DEPC) ultrapure water. The dNTP solution, UltraPure diethyl pyrocarbonate (DEPC)-treated water, and high-performance liquid chromatography (HPLC)-purified DNA and miRNA sequences were purchased from Sangon Biotechnology Co. Ltd. (Shanghai, China). The base sequences are shown in Table S1 in the Electronic Supplementary Material (ESM). The human liver cancer HepG2 cell line was obtained from the Chinese Academy of Sciences Cell Bank. HepG2 cells were cultured in Dulbecco's modified Eagle's medium (DMEM) supplemented with 10% (*v*/v) FBS and incubated at 37 °C in a humidified atmosphere containing 5% CO_2.

Instruments

Fluorescence analysis was performed using the PerkinElmer LS-55 Fluorescence Spectrophotometer (PerkinElmer, UK) with voltage set to 750 V and slit width to 10 nm. The excitation and emission wavelengths used were 350 nm and 600 nm, respectively. Gel electrophoresis analysis was performed using the DYY-6C electrophoresis apparatus (Liuyi Instrument Factory, China). Morphological characterization was performed with a Talos F200S transmission electron microscope.

Solution preparation

HP1, HP2, and HP3 DNA were dissolved to 20 μmol/L in 10 mmol/L Tris-HAc buffer and heated at 90 °C for 10 min. The DNA was then slowly cooled to room temperature in order to form a stable hairpin structure. MiRNA-122 was dissolved in DEPC-treated water to a final concentration of 20 μmol/L, stored at −20 °C in the dark, and diluted to the required concentration when needed.

Fluorescence-based miRNA assays

First, 0.05 μmol/L HP1, 0.3 μmol/L HP2, 0.3 μmol/L HP3, 30 μmol/L dNTPs, 2 U KF, and various concentrations of target miRNA-122 solution were combined in a centrifuge tube, and diluted with 1X NEB buffer to 50 μL. The solution was then placed in the dark for 1 min, and then incubated at 37 °C for 3 h in the dark. After polymerisation was completed, 400 μmol/L Cu^{2+} and 4 mmol/L ascorbic acid were added, and the volume was adjusted to 200 μL with MOPS buffer.[6] Finally, the reaction was carried out for 10 min at room temperature and the fluorescence spectra of the solutions were recorded.

Preparation of cell lysates

In this study, hepatocellular carcinoma HepG2 cell lysates were used for complex sample analysis. The cells were dispersed in 10 mmol/L Tris-HCl buffer, followed by ultrasonication for 10 min and centrifugation at 8000 rpm for 1 min. The supernatant was then obtained and centrifuged in a 10 kD ultrafiltration centrifuge tube at 4 °C for 30 min. Finally, the filtrate was collected for further use.

Gel electrophoresis

Gels were prepared with 5% agarose and 1X Tris/borate/EDTA (TBE) running buffer. The sample was added to the agarose gel, quickly placed in an electrophoresis tank, and run for 90 min at 100 V [43]. Finally, the gel was placed in ethidium bromide solution for 30 min and photographed using the Omega-16ic imaging system (Ultra-Lum, US).

Results and discussion

Principles of the miRNA detection strategy

We used miRNA-122 as the target during development of this assay. The design of the assay is shown in Fig. 1. Three types DNA hairpin probes, HP1, HP2, and HP3, were designed. The 3′ overhang and stem part of HP1 are the recognition sequence of miRNA-122, and the blue regions of HP1 and HP2 have complementary base pairing. The pink regions of HP2 and HP3 are also complementary. The overhangs and loops of HP2 and HP3 are rich in A-T bases and act as templates for polymerisation to generate long dsDNA rich in A-T base pairs. In the absence of miRNA-122, the complementary regions of HP1, HP2, and HP3 are closed and cannot access each other. Under these conditions, when Cu^{2+} and ascorbic acid are added, the fluorescence signal of the system is weak due to the absence of A-T bases pairs. When miRNA-122 is present, it hybridises with HP1 to form a DNA-RNA complex, which releases the 5′ blue region of HP1 to hybridise with the blue region of HP2. At this time, the pink portion of HP2 is released and binds to the pink portion of the 3′ end of HP3. In the presence of polymerase, this miRNA/HP1/HP2/HP3 structure is polymerised from the 3′ to the 5′ end, forming dsDNA rich in A-T base pairs [9]. As hybridisation and polymerisation progress, the dsDNA template for CuNPs is formed. After completion of this reaction, Cu^{2+} and ascorbic acid are added to form CuNPs with high fluorescence intensity. Therefore, detection and analysis of miRNA-122 can be achieved through DNA-RNA binding cycles and signal amplification by polymerase.

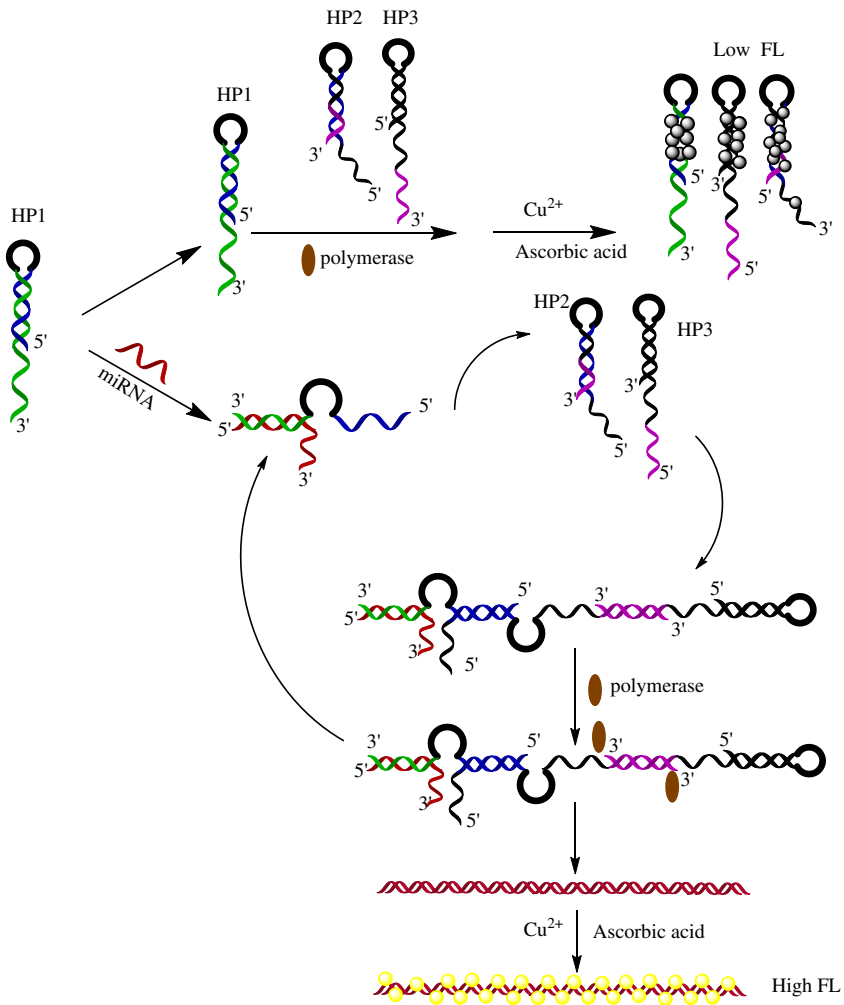

Fig. 1 Analysis of miRNA-122 based on enzyme-assisted signal amplification and DNA-CuNP fluorescence enhancement sensing method

Feasibility of the detection strategy

In order to assess the feasibility of this method, we measured the fluorescence spectra of dsDNA-CuNPs and formation of dsDNA under different experimental conditions by agarose gel electrophoresis. The fluorescence spectra of the dsDNA-CuNPs are shown in Fig. S10 (see ESM). When the target is absent, the fluorescence excitation and emission peaks of the system are very low due to its inability to initiate polymerisation (ESM Fig. S10 c and d). When the target miRNA-122 is present in the system, the polymerisation reaction is initiated, forming a dsDNA template for dsDNA-CuNPs. As shown in Fig. S10a and b (see ESM), the excitation and emission wavelengths of the dsDNA-CuNPs formed by this system are 352 nm and 600 nm, respectively.

The fluorescence emission spectra of the system are shown in Fig. 2. When no target is present, the complementary regions of HP1, HP2, and HP3 are masked. Under these conditions, KF cannot initiate polymerisation and dsDNA template formation, so the fluorescence of the CuNPs formed after the addition of Cu^{2+} and ascorbic acid is very low (Fig. 2a and c). When the target is present in the system but KF is absent, the polymerisation reaction is still inhibited, and the fluorescence of the system is very low (Fig. 2b). If the target is present, the polymerisation reaction is initiated and a large amount of dsDNA template is formed. After adding Cu^{2+} and ascorbic acid, the system forms dsDNA-CuNPs and has high fluorescence intensity (Fig. 2d). These results indicate that the system can successfully complete RNA-DNA complex circulation by enzyme-assisted signal amplification for the analysis and detection of miRNA-122. In addition, we used transmission electron microscopy (TEM) to carry out the morphological characterization of CuNPs (see ESM Fig. S9). The results showed that the copper nanoparticles were synthesized with good dispersion and particle size of about 5 nm. The above results indicate that the copper nanoparticles were successfully synthesized in the system after the addition of the target.

In addition, we assessed the formation of long dsDNA in this assay by agarose gel electrophoresis. The results are shown in Fig. 3. The positions of the two bright bands in lane 4 (HP1, HP2, and HP3) were nearly identical to those in lanes 1 (HP1 alone), 2 (HP2 alone), and 3 (HP3 alone), indicating that HP1, HP2, and HP3 do not hybridise in the absence of the target. Also, the bright bands in lane 6 (HP1, HP2, HP3, and KF) were the same as in lane 4, showing that KF cannot initiate polymerisation spontaneously. Most importantly, a new large molecular weight band appeared in lane 5 (HP1, HP2, HP3, KF, and miR-122), and the bands corresponding to HP1, HP2, and HP3 decreased, indicating that the polymerisation reaction was initiated in the presence of miR-122 by the action of KF. This provides further evidence of the feasibility of this target detection method.

Optimisation of assay conditions

In order to obtain the highest sensitivity in detecting miR-122, we optimised conditions including the concentrations of HP1, HP2, HP3, KF, Cu^{2+}, ascorbic acid, and dNTPs, as well as the cyclic polymerisation time.

The HP1 concentration has a large influence on the recognition of the target miRNA-122 through its hybridisation efficiency. The prominent single-stranded and loop portions of HP2 and HP3 are rich in A or T bases, which affect the polymerization and generation of the dsDNA-CuNPs templates in the system, resulting in variations in the fluorescence signal of the system.

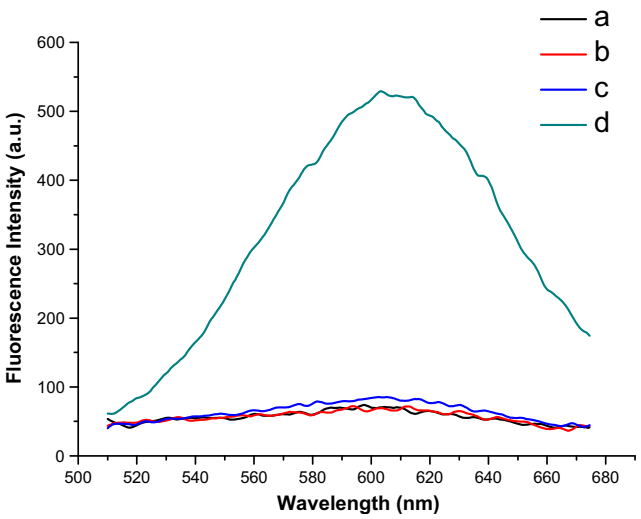

Fig. 2 Fluorescence emission spectra of the system under different experimental conditions. (**a**) HP1 + HP2 + HP3; (**b**) HP1 + HP2 + HP3 + miRNA-122; (**c**) HP1 + HP2 + HP3+ KF; (**d**) HP1 + HP2 + HP3+ miRNA-122+ KF

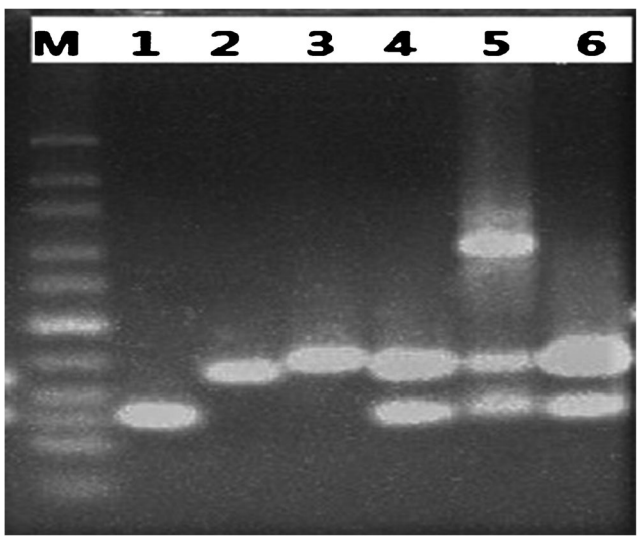

Fig. 3 Agarose gel electrophoresis of reactions containing components of the system. Lane M: DNA marker 1: HP1; 2: HP2; 3: HP3; 4: HP1 + HP2 + HP3; 5: HP1 + HP2 + HP3 + miRNA-122 + KF; 6: HP1 + HP2 + HP3 + KF

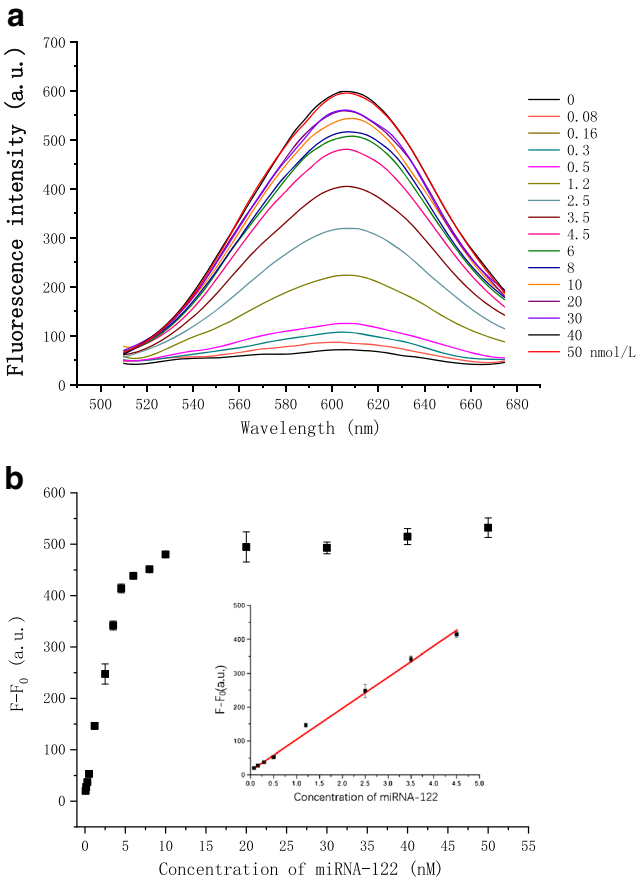

Fig. 4 (**a**) Fluorescence emission spectra in the presence of different concentrations of miRNA-122. (**b**) The linear relationship between $F\text{-}F_0$ and concentration of miR-122 in the range of 80.0 pmol/L to 4.50 nmol/L. The inset is the working curve for miRNA-122 ($n = 3$)

Therefore, we first optimised the concentrations of HP1, HP2, and HP3. As measured by the maximal fluorescence change value ($F\text{-}F_0$) and change ratio (F/F_0), the optimal concentrations of HP1, HP2, and HP3 were 0.05 μmol/L, 0.3 μmol/L, and 0.3 μmol/L, respectively (see ESM Figs. S1, S2, and S3).

This method is based on the ability of polymerase to generate a large number of dsDNA templates to form dsDNA-CuNPs with high fluorescence intensity. The RNA-DNA complex acts as a circulator, and the cyclic polymerisation time of the system has a large influence on the fluorescence signal output. Additionally, KF and dNTPs are required for polymerisation, and the unnecessary excess KF and dNTPs will result in nonspecific polymerization. Therefore, we also optimised their concentrations. The optimum KF dosage was 2 U, and the optimal concentration of dNTPs was 30 μmol/L; the optimal cycle polymerisation time was 3 h (see ESM Figs. S4, S5, and S6).

The fluorescence signal output of the system is also highly dependent on the fluorescence of the CuNPs formed by the dsDNA templates. The concentration of Cu^{2+} and the reducing agent ascorbic acid have a direct influence on the formation of fluorescent CuNPs. Therefore, we optimised the Cu^{2+} and ascorbic acid concentrations, and the results are shown in Figs. S7 and S8 (see ESM). The redundant Cu^{2+} and ascorbic acid will result in decreased fluorescence intensity of CuNPs, because in the presence of excess Cu^{2+} and ascorbic acid, aggregation of the CuNPs can occur. According to our analysis, the optimal concentrations of Cu^{2+} and ascorbic acid are 0.4 mmol/L and 2 mmol/L, respectively.

Analytical performance of the detection method

Under the previously determined optimal conditions, we explored the analytical performance of the method for the detection of target miRNA-122. As shown in Fig. 4a, as the concentration of target miRNA-122 increased, the fluorescence intensity of the dsDNA-CuNPs also increased. Figure 4b shows a plot of the change in fluorescence signal intensity by miRNA-122 concentration, and the inset depicts the working curve for miRNA-122. The fluorescence change value ($F\text{-}F_0$) was linear in the range 80.0 pmol/L to 4.50 nmol/L miRNA-122. The

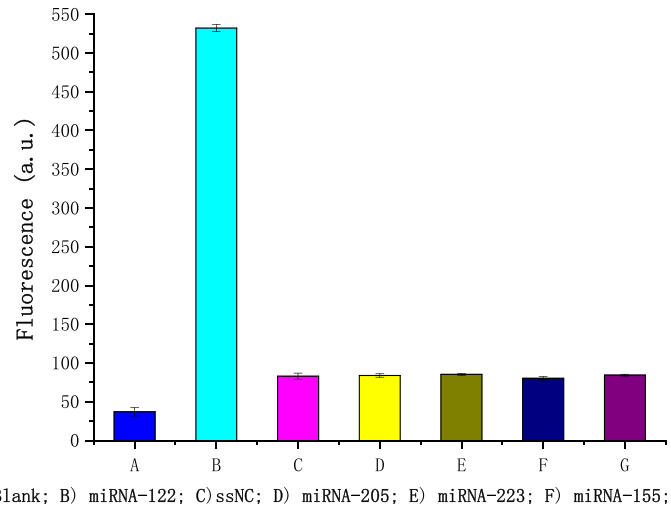

Fig. 5 Fluorescence intensity of the system in the presence of non-target miRNAs and a random sequence ($n = 3$)

Table 1 The recovery of miRNA-122 in spiked hepatoma HepG2 cell lysate samples ($n = 3$)

Sample	Spiked (nmol/L)	Recovered[a] (nmol/L)	Recovery%	RSD% ($n = 3$)
1	0.160	0.164 ± 0.056	102.53	5.35
2	1.20	1.12 ± 0.075	93.33	4.73
3	3.00	2.87 ± 0.14	95.67	0.59

[a] (±) is the uncertainty of the concentration for the samples

linear equation was: $(F\text{-}F_0) = 92.53C + 11.18$ ($R^2 = 0.9927$). According to the limit of detection (LOD = 3σ/k, where σ is the standard deviation of multiple blanks, and k is the slope of the standard curve), the detection limit of miRNA-122 in this assay is approximately 17.8 pmol/L. Compared with other available methods, the sensitivity of our method is slightly improved (see ESM Table S2) [10].

Selectivity of the detection method

Under the optimal assay conditions, we evaluated the detection of other non-target miRNAs (miRNA-21, miRNA-155, miRNA-221, and miRNA-223) related to hepatitis C or liver cancer and a random sequence to investigate the selectivity of our system. The experimental results are shown in Fig. 5. The polymerisation cycle reaction was initiated only when miRNA-122 was present in the system and resulted in a significant increase in fluorescence. The other miRNAs did not affect the fluorescence signal of the system, even when their concentrations were 50 times that of the target. The above results indicate that this method has good selectivity for the detection of its target miRNA.

Application of the system to complex samples

In order to investigate the detection performance of this assay in biologically relevant complex samples, we performed spike-and-recovery experiments in hepatoma HepG2 cell lysates. The results are shown in Table 1, and the measured spiked recovery has a relative standard deviation (RSD) of about 5%. These results demonstrate that this method can be applied to complex samples for detection and analysis of target miRNAs [44].

Conclusion

We developed a label-free dsDNA-CuNP-based, enzyme-assisted signal amplification method for the detection of microRNA. This method utilises polymerase and RNA-DNA complex circulation to generate large numbers of DNA duplexes that serve as templates for the formation of highly fluorescent CuNPs. The method has the desirable characteristics of no labelling, simple and mild conditions, and sensitive and selective detection. The detection limit for miR-122 is 17.8 pmol/L. In addition, the method can accurately detect miRNA-122 spiked in hepatoma HepG2 cell lysates.

Acknowledgements This work was supported by the National Natural Science Foundation of China (nos. 21465007, 21565007, 21165004, 21163002), the Guangxi Natural Science Foundation of China (2015GXNSFGA139003), Bagui group of Guangxi province, and the project of State Key Laboratory for Chemistry and Molecular Engineering of Medicinal Resources, School of Chemistry and Pharmaceutical Science of Guangxi Normal University (CMEMR2014-A08).

Compliance with ethical standards

Conflict of interest The authors declare that they have no conflict of interest.

References

1. Bartel DP. MicroRNAs: genomics, biogenesis, mechanism, and function. Cell. 2004;116:281–91.
2. Zeng Y, Wagner EJ, Cullen BR. Both natural and designed microRNAs can Inhibit the expression of cognate mRNAs when expressed in human cells. Mol Cell. 2002;9:1327–33.
3. Volinia S, Calin GA, Liu CG, Ambs S, Cimmino A, Petrocca F, et al. A microRNA expression signature of human solid tumors defines cancer gene targets. Proc Natl Acad Sci U S A. 2006;103(7):2257–61.
4. Tian T, Wang J, Zhou X. A review: microRNA detection methods. Organic Biomol Chem. 2015;13(8):2226–38.
5. Li J, Tan S, Kooger R, Zhang C, Zhang Y. MicroRNAs as novel biological targets for detection and regulation. Chem Soc Rev. 2014;43(2):506–17.
6. Xu Y, Wang Y, Liu S, Yu J, Wang H, Guo Y, et al. Ultrasensitive and rapid detection of miRNA with three-way junction structure-based trigger-assisted exponential enzymatic amplification. Biosens Bioelectron. 2016;81:236–41.
7. He YC, Yin BC, Jiang L, Ye BC. The rapid detection of microRNA based on p19-enhanced fluorescence polarization. Chem Commun (Camb). 2014;50(47):6236–9.
8. Yan H, Bhattarai U, Guo ZF, Liang FS. Regulating miRNA-21 biogenesis by bifunctional small molecules. J Am Chem Soc. 2017;139(14):4987–90.
9. Xu F, Shi H, He X, Wang K, He D, Guo Q, et al. Concatemeric dsDNA-templated copper nanoparticles strategy with improved sensitivity and stability based on rolling circle replication and its application in microRNA detection. Anal Chem. 2014;86(14):6976–82.

10. Wei J, Gong X, Wang Q, Pan M, Liu X, Liu J, et al. Construction of an autonomously concatenated hybridization chain reaction for signal amplification and intracellular imaging. Chem Sci. 2018;9(1):52–61.
11. Wang H-B, Zhang H-D, Chen Y, Liu Y-M. Inhibition of double-stranded DNA templated copper nanoparticles as label-free fluorescent sensors for L-histidine detection. New J Chem. 2015;39(11):8896–900.
12. Zhang H, Lin Z, Su X. Label-free detection of exonuclease III by using dsDNA-templated copper nanoparticles as fluorescent probe. Talanta. 2015;131:59–63.
13. Zhou Z, Du Y, Dong S. Double-strand DNA-templated formation of copper nanoparticles as fluorescent probe for label-free aptamer sensor. Anal Chem. 2011;83(13):5122–7.
14. Du Y, Dong S. Nucleic acid biosensors: recent advances and perspectives. Anal Chem. 2017;89(1):189–215.
15. Yan L, Zhou J, Zheng Y, Gamson AS, Roembke BT, Nakayama S, et al. Isothermal amplified detection of DNA and RNA. Mol BioSyst. 2014;10(5):970.
16. Cheng Y, Dong L, Zhang J, Zhao Y, Li Z. Recent advances in microRNA detection. Analyst. 2018;143(8):1758–74.
17. Gerasimova YV, Kolpashchikov DM. Enzyme-assisted target recycling (EATR) for nucleic acid detection. Chem Soc Rev. 2014;43(17):6405–38.
18. Ahrberg CD, Manz A, Chung BG. Polymerase chain reaction in microfluidic devices. Lab Chip. 2016;16(20):3866–84.
19. Li J, Yao B, Huang H, Wang Z, Sun CH, Fan Y, et al. Real-time polymerase chain reaction microRNA detection based on enzymatic stem-loop probes ligation. Anal Chem. 2009;81(13):5446–51.
20. Ali MM, Li F, Zhang Z, Zhang K, Kang DK, Ankrum JA, et al. Rolling circle amplification: a versatile tool for chemical biology, materials science and medicine. Chem Soc Rev. 2014;43(10):3324–41.
21. Zhou F, Li B, Ma J. A linear DNA probe as an alternative to a molecular beacon for improving the sensitivity of a homogenous fluorescence biosensing platform for DNA detection using target-primed rolling circle amplification. RSC Adv. 2015;5(6):4019–25.
22. Ge J, Zhang L-L, Liu S-J, Yu R-Q, Chu X. A highly sensitive target-primed rolling circle amplification (TPRCA) method for fluorescent in situ hybridization detection of microRNA in tumor cells. Anal Chem. 2014;86(3):1808–15.
23. Cui L, Zhu Z, Lin N, Zhang H, Guan Z, Yang CJ. A T7 exonuclease-assisted cyclic enzymatic amplification method coupled with rolling circle amplification: a dual-amplification strategy for sensitive and selective microRNA detection. Chem Commun (Camb). 2014;50(13):1576–8.
24. Gu Y, Song J, Li M-X, Zhang T-T, Zhao W, Xu J-J, et al. Ultrasensitive microRNA assay via surface plasmon resonance responses of au@Ag Nanorods etching. Anal Chem. 2017;89(19):10585–91.
25. Li L, Feng J, Liu H, Li Q, Tong L, Tang B. Two-color imaging of microRNA with enzyme-free signal amplification via hybridization chain reactions in living cells. Chem Sci. 2016;7(3):1940–5.
26. Tang Y, Lu B, Zhu Z, Li B. Establishment of a universal and rational gene detection strategy through three-way junction-based remote transduction. Chem Sci. 2018;9(3):760–9.
27. Kim D, Wei Q, Kim DH, Tseng D, Zhang J, Pan E, et al. Enzyme-free nucleic acid amplification assay using a cellphone-based well plate fluorescence reader. Anal Chem. 2018;90(1):690–5.
28. Yi JT, Chen TT, Huo J, Chu X. Nanoscale zeolitic imidazolate framework-8 for ratiometric fluorescence imaging of MicroRNA in living cells. Anal Chem. 2017;89(22):12351–9.
29. Liu JL, Tang ZL, Zhuo Y, Chai YQ, Yuan R. Ternary electrochemiluminescence system based on rubrene microrods as luminophore and Pt nanomaterials as coreaction accelerator for ultrasensitive detection of MicroRNA from cancer cells. Anal Chem. 2017;89(17):9108–15.
30. Ye S, Li X, Wang M, Tang B. Fluorescence and SERS imaging for the simultaneous absolute quantification of multiple miRNAs in living cells. Anal Chem. 2017;89(9):5124–30.
31. Duan R, Lou X, Xia F. The development of nanostructure assisted isothermal amplification in biosensors. Chem Soc Rev. 2016;45(6):1738–49.
32. Xu S, Nie Y, Jiang L, Wang J, Xu G, Wang W, et al. Polydopamine nanosphere/gold nanocluster (au NC)-based nanoplatform for dual color simultaneous detection of multiple tumor-related MicroRNAs with DNase-I-assisted target recycling amplification. Anal Chem. 2018;90(6):4039–45.
33. Sun J, Pi F, Ji J, Lei H, Gao Z, Zhang Y, et al. Ultrasensitive "FRET-SEF" probe for sensing and imaging MicroRNAs in living cells based on gold nanoconjugates. Anal Chem. 2018;90(5):3099–108.
34. Qu X, Jin H, Liu Y, Sun Q. Strand displacement amplification reaction on quantum dot-encoded silica bead for visual detection of multiplex MicroRNAs. Anal Chem. 2018;90(5):3482–9.
35. Yuan R, Yu X, Zhang Y, Xu L, Cheng W, Tu Z, et al. Target-triggered DNA nanoassembly on quantum dots and DNAzyme-modulated double quenching for ultrasensitive microRNA biosensing. Biosens Bioelectron. 2017;92:342–8.
36. Zheng Y-N, Liang W-B, Xiong C-Y, Zhuo Y, Chai Y-Q, Yuan R. Universal ratiometric photoelectrochemical bioassay with target-nucleotide transduction-amplification and electron-transfer tunneling distance regulation strategies for ultrasensitive determination of microRNA in cells. Anal Chem. 2017;89(17):9445–51.
37. Liu Q, Ma C, Liu XP, Wei YP, Mao CJ, Zhu JJ. A novel electrochemiluminescence biosensor for the detection of microRNAs based on a DNA functionalized nitrogen doped carbon quantum dots as signal enhancers. Biosens Bioelectron. 2017;92:273–9.
38. Chi BZ, Liang RP, Qiu WB, Yuan YH, Qiu JD. Direct fluorescence detection of microRNA based on enzymatically engineered primer extension poly-thymine (EPEPT) reaction using copper nanoparticles as nano-dye. Biosens Bioelectron. 2017;87:216–21.
39. Miao P, Zhang T, Xu J, Tang Y. Electrochemical detection of miRNA combining T7 exonuclease-assisted cascade signal amplification and DNA-templated copper nanoparticles. Anal Chem. 2018;90(18):11154–60.
40. Mao Z, Qing Z, Qing T, Xu F, Wen L, He X, et al. Poly(thymine)-templated copper nanoparticles as a fluorescent Indicator for hydrogen peroxide and oxidase-based biosensing. Anal Chem. 2015;87(14):7454–60.
41. Chen J, Ji X, He Z. Smart composite reagent composed of double-stranded DNA-templated copper nanoparticle and SYBR green I for hydrogen peroxide related biosensing. Anal Chem. 2017;89(7):3988–95.
42. Qing Z, Bai A, Xing S, Zou Z, He X, Wang K, et al. Progress in biosensor based on DNA-templated copper nanoparticles. Biosens Bioelectron. 2019;137:96–109.
43. Liu MX, Liang S, Tang Y, Tian J, Zhao Y, Zhao S. Rapid and label-free fluorescence bioassay for microRNA based on exonuclease III-assisted cycle amplification. RSC Adv. 2018;8(29):15967–72.
44. Tang Y, Liu M, Xu L, Tian J, Yang X, Zhao Y, et al. A simple and rapid dual-cycle amplification strategy for microRNA based on graphene oxide and exonuclease III-assisted fluorescence recovery. Anal Methods. 2018;10(30):3777–82.